Improved methods for dewarping images in convex mirrors in fine art: Applications to van Eyck and Parmigianino

Yumi Usami,[a] David G. Stork,[b] Jun Fujiki,[c]
Hideitsu Hino,[a] Shotaro Akaho,[c] and Noboru Murata[a]

[a]Waseda University, Okubo 3-4-1, Shinjuku-ku, Tokyo, 169-8555 JAPAN
[b]Ricoh Innovations, 2882 Sand Hill Road Suite 115, Menlo Park CA 94025 USA
[c]National Institute of Advanced Industrial Science and Technology,
Tsukuba, Ibaraki, 305-8568 JAPAN

ABSTRACT

We derive and demonstrate new methods for dewarping images depicted in convex mirrors in artwork and for estimating the three-dimensional shapes of the mirrors themselves. Previous methods were based on the assumption that mirrors were spherical or paraboloidal, an assumption unlikely to hold for hand-blown glass spheres used in early Renaissance art, such as Johannes van Eyck's *Portrait of Giovanni (?) Arnolfini and his wife* (1434) and Robert Campin's *Portrait of St. John the Baptist and Heinrich von Werl* (1438). Our methods are more general than such previous methods in that we assume merely that the mirror is radially symmetric and that there are straight lines (or colinear points) in the actual source scene. We express the mirror's shape as a mathematical series and pose the image dewarping task as that of estimating the coefficients in the series expansion. Central to our method is the *plumbline principle*: that the optimal coefficients are those that dewarp the mirror image so as to straighten lines that correspond to straight lines in the source scene. We solve for these coefficients algebraically through principal component analysis, PCA. Our method relies on a global figure of merit to balance warping errors throughout the image and it thereby reduces a reliance on the somewhat subjective criterion used in earlier methods. Our estimation can be applied to separate image annuli, which is appropriate if the mirror shape is irregular. Once we have found the optimal image dewarping, we compute the mirror shape by solving a differential equation based on the estimated dewarping function. We demonstrate our methods on the *Arnolfini* mirror and reveal a dewarped image superior to those found in prior work—an image noticeably more rectilinear throughout and having a more coherent geometrical perspective and vanishing points. Moreover, we find the mirror deviated from spherical and paraboloidal shape; this implies that it would have been useless as a concave projection mirror, as has been claimed. Our dewarped image can be compared to the geometry in the full *Arnolfini* painting; the geometrical agreement strongly suggests that van Eyck worked from an actual room, not, as has been suggested by some art historians, a "fictive" room of his imagination. We apply our method to other mirrors depicted in art, such as Parmigianino's *Self-portrait in a convex mirror* and compare our results to those from earlier computer graphics simulations.

Keywords: convex mirror in art, Johannes van Eyck, *Arnolfini portrait*, Parmigianino, *Self portrait in a convex mirror*, computer vision and art, image dewarping, principal component dewarping

1. INTRODUCTION

Convex mirrors begin to appear in art of the early Renaissance, especially in the Low Countries, such as Johannes van Eyck's *Portrait of Giovanni (?) Arnolfini and his wife* (1434), Robert Campin's *Portrait of St. John the Baptist and Heinrich von Werl* (1438), among several others. Criminisi, Kemp and Kang modeled such mirrors as sections of spheres or paraboloids and adjusted the single-parameter dewarping transformations until the image "looked best" to reveal new views into the tableaus of these artists.[1] Such dewarped images can be tested for geometric coherence and vanishing points, and compared to the actual room as depicted throughout the painting. The relative sizes of figures in the dewarped image could be estimated as well. Stork exploited such

Send correspondence to David G. Stork, artanalyst@gmail.com.

methods to estimate the radius of curvature, R, of the celebrated Arnolfini mirror to then computed its focal length, $f = R/2$.[2–5] Because this focal length differed significantly from that of a mirror consistent with the full image itself, he could refute the claim by David Hockney and Charles Falco that "van Eyck placed a convex mirror at the center of this [Arnolfini] masterpiece, *the very mirror* which, turned around, he may well have used to construct the image"(emphasis added).[6] Savarese et al. modelled the convex mirror in Hans Memling's *Virgin and Child with Maarten van Nieuwenhove* (1487) as a section of a sphere and used computer graphics reconstruction of the tableau and mirror to test whether the mirror was added by the artist as an afterthought.[7] Stork and Furuichi built a full three-dimensional computer graphics model of Parmigianino's studio—including the convex "barber's mirror," described by Vasari—to test whether the painting corresponded closely to the image of a rectilinear room reflected in a convex mirror of a plausible radius of curvature.[8]

While there have been a number of methods for dewarping images in specular surface under different conditions and inferring the shape of the associated mirror surface,[9] the prior algorithms for dewarping images in old master *art* suffer from two important limitations:

- Such methods are applicable to mirrors of the form assumed, specifically spheres and paraboloids. In fact, convex mirrors—especially hand-blown glass mirrors of the Renaissance—need not conform to these simple geometric or optical forms. Such previous dewarping methods are too limited to dewarp images in the general case and are not capable of *revealing* the optimal shape, should this shape differ from some assumed general form.
- Previous methods judged dewarping by eye, not by an objective global figure of merit. When there is no "perfect" dewarping, there may be no simple method to subjectively weight the penalty of distortions throughout the image, such as incompletely corrected line segments of different lengths, orientations, and positions.

We apply extensions to methods from panoramic camera calibration, developed by Hino et al.[10] and Jujiki et al.,[11] to this problem of dewarping images in convex mirrors in art so as to overcome these two limitations. In Sect. 2 we review the background of dewarping in this context and the theory of our method. Then in Sect. 3 we show how to merge or interpolate dewarping functions defined on different annular regions. In Sect. 4 we describe the mathematics underlying the reconstruction of the mirror shape from the dewarping function. In Sect. 5 we demonstrate and validate our methods by testing them on a photograph of a modern convex mirror. Section 6 contains our central contributions; we apply our method to dewarping images in two important art works of the western canon. We find that our dewarped images for the *Arnolfini portrait* are superior to those of previous work, specifically that perspective lines agree more closely at vanishing points. We then reveal the most likely shape of Arnolfini's mirror and re-estimate its focal length in order to consider more carefully the claim by Hockney and Falco that the mirror could have been turned around and used as a concave projection mirror to create the full image in the painting. We conclude in Sect. 7 by describing future technical refinements and possible applications elsewhere in art historical research.

2. PRINCIPAL COMPONENT DEWARPING

We address the problem of estimating the non-linear mapping between points in the observation plane to points in a convex mirror. We assume the distortion is centered in the mirror and purely radial, that is, depends solely on the distance to the mirror's optical axis. We let r represent the scaled distance between a two-dimensional point $\mathbf{x}$ and the center in the distorted observation plane, and let $f(r)$ represent the distance in the undistorted plane. We model this function by a linear combination of N basis functions; therefore the dewarping problem corresponds to estimating the associated N coefficients. This estimation problem can be formulated as a linear fitting problem in the perspective projection plane and reduced to eigenvalue problems, as we shall see.

We denote a point in the source space as $\mathbf{x}$ and its corresponding perspective projection plane by $\boldsymbol{\phi}(\mathbf{x})$. Under the assumption of radially symmetric distortion, the mapping $\boldsymbol{\phi}(\mathbf{x})$ can be represented as a function $f(r)$, which depends only on the radius r:

$$\boldsymbol{\phi}(\mathbf{x}) = f(r)\frac{\mathbf{x}}{\|\mathbf{x}\|} = \frac{f(r)}{r}\mathbf{x}, \tag{1}$$

where $\|\mathbf{x}\| = r$, as shown in Fig. 1. We approximate the calibration function using a linear combination of basis functions as

$$f(r) = \sum_{n=1}^{N} c_n f_n(r), \tag{2}$$

and thus the dewarping task corresponds to estimating the N coefficients $\mathbf{c} = (c_1, \ldots, c_N)^t$ using image data.[10]

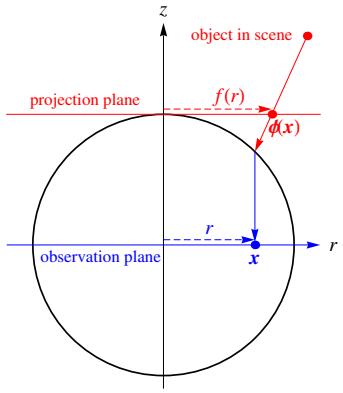

Figure 1. A two-dimensional slice of the camera sphere showing our notation: a point $\mathbf{x}$ a distance r on the observation plane corresponds to a point on the projection plane a distance $f(r)$ from the optical axis. The nonlinear mapping $f(r)$ depends upon the shape of the convex mirror and the task of dewarping is to estimate this function and apply it to the image.

Many real three-dimensional scenes, such as the interiors of rooms depicted in Renaissance art, contain a number of straight lines, and these lines appear distorted in the convex mirror. We suppose that there are S such lines in the observation plane, and denote data points on each of those lines as $\{\mathbf{x}_{[d]}^s\}_{d=1}^{D_s}, s = 1, \ldots, S$. We also suppose that S is greater than the number of bases of the calibration function, N. Our task, then, is to estimate the coefficient vector $\mathbf{c}$ of the calibration function, Eq. 2 based on the information from the lines.

We first consider D points on a single straight line in the scene, $\{\mathbf{x}_{[d]}\}_{d=1}^{D}$ and map each point as

$$\boldsymbol{\phi}(\mathbf{x}_{[d]}) = \sum_{n=1}^{N} c_n\, \boldsymbol{\phi}_n(\mathbf{x}_{[d]}) = P(\mathbf{x}_{[d]})\mathbf{c}, \tag{3}$$

where each basis function is $\boldsymbol{\phi}_n(\mathbf{x}) = f_n(\|\mathbf{x}\|)\mathbf{x}/\|\mathbf{x}\|$ and

$$P(\mathbf{x}_{[d]}) \equiv \left(\boldsymbol{\phi}_1(\mathbf{x}_{[d]}), \ldots, \boldsymbol{\phi}_N(\mathbf{x}_{[d]})\right). \tag{4}$$

Our *plumbline principle* demands that all the D points $\boldsymbol{\phi}(\mathbf{x}_{[d]})$ lie on the same line, and this leads to the D constraints

$$\mathbf{a}^t\boldsymbol{\phi}(\mathbf{x}_{[d]}) + b = \mathbf{a}^t P(\mathbf{x}_{[d]})\mathbf{c} + b = \mathbf{c} \otimes \mathbf{a}^t \mathrm{Span}[P(\mathbf{x}_{[d]})] + b = 0, \tag{5}$$

where $\mathbf{a}$ is the normal vector, b the scalar intercept of the line, Span[$\mathbf{X}$] the column span of a matrix $\mathbf{X}$, and $\otimes$ the vector cross product. We rewrite Eq. 5 as

$$\left(\mathbf{\Phi}(\mathbf{x}_{[1]}) \ \ldots \mathbf{\Phi}(\mathbf{x}_{[D]})\right)^t \mathbf{C} = \mathbf{0}_D, \tag{6}$$

where $\mathbf{0}_D$ denotes the D-dimensional vector of 0s,

$$\mathbf{\Phi}(\mathbf{x}) = \left(\text{Span}[\text{P}(\mathbf{x})]^{\text{t}} \ 1\right)^t \text{and } \mathbf{C} = \left((\mathbf{c} \otimes \mathbf{a})^{\text{t}} \ 1\right)^{\text{t}}. \tag{7}$$

Real, sensed images inevitably contain noise and thus Eq. 5 can hold only approximately. For this reason, we incorporate regularization into our minimum-square-error optimization problem, which is then expressed

$$\min_{\mathbf{C}} \mathbf{C}^t \mathbf{\Phi} \mathbf{\Phi}^t \mathbf{C} \quad \text{subject to } \|\mathbf{C}\| = 1. \tag{8}$$

Its solution is given by the unit eigenvector of a matrix $\mathbf{\Phi}\mathbf{\Phi}^t$ corresponding to the minimum eigenvalue.[12] We solve Eq. 8 for each of the S lines and get S estimates with common $\mathbf{C}$. Through a straightforward derivation stemming from the definitions in Eq. 7, this optimization can be recast in terms of $\mathbf{c}$.[10] Once we have estimated this vector of coefficients, we use it in Eq. 2 to dewarp the image.

The above method is valid regardless of the set of smooth, continuous basis functions, and thus the choice of basis function is up to the experimenter. We find that a linear term works well, while additional terms depend upon the image in question or the assumed mirror shape; for instance, a spherical mirror has a warping function of the following exact form and Taylor series:

$$f_n(r) = \frac{r - 2r\sqrt{1 - r^2}}{2r^2 - 1} = r + r^3 + \frac{7}{4}r^5 + O(r^7). \tag{9}$$

Principled statistical guidelines for selecting basis functions is a topic of future research (Sect. 7).

3. INTERPOLATING SEGMENTED DEWARPING FUNCTIONS

If the mirror shape is simple throughout, then a single, appropriately chosen warping function $f(r)$ may suffice to give an accurate dewarping of the image. If however the mirror is irregular, such as a hand-blown glass mirror from the Renaissance, then a more complicated model may be needed, for instance different dewarping functions in different annular regions of the image. To this end we divide the image area into several annular regions according to the distance from the image center, estimate each dewarping function to suit each annular region and then interpolate these functions so as to cover the whole image.

The central challenge of this method is to connect each patch of estimated functions and make the boundary smooth. We apply a Gaussian smoothing and interpolation method to this end. Recall that a one-dimensional Gaussian or normal distribution is given by

$$N(r; r_0, \sigma) = \frac{1}{\sqrt{2\pi}\sigma} \exp\left(-\frac{(r - r_0)^2}{2\sigma^2}\right). \tag{10}$$

Suppose there are m different estimated functions: $f_1(r), \ldots, f_m(r)$, each corresponding to abutting disjoint annular regions in the image. The relative weighting of the Gaussian functions to cover $f_k(r)$ for $k = 1, \ldots, m$ is then given by

$$g_k(r) = \frac{N(r; r_k, \sigma_k)}{\sum_{i=1}^{m} N(r; r_i, \sigma_i)}, \tag{11}$$

and the full dewarping function is constructed by connecting m estimated functions weighted by Gaussians, i.e.,

$$f(r) = \sum_{i=1}^{m} g_i(r) f_i(r). \tag{12}$$

We demand, further, that the full dewarping function be continuous and monotonically increasing, since it marks the length from the center of the image on the transformed image.[10] We compute the scale of each function so as to satisfy $f_k(r_k) = f_{k+1}(r_k)$ for $k = 1, \ldots, m-1$, when we concatenate f_k and f_{k+1} at the circular boundary corresponding to $r = x_k$.

4. RECONSTRUCTING THE MIRROR SURFACE

Once we have estimated the dewarping function, $f(r)$, we can compute the the cross section of the three-dimensional shape of the mirror, $S(r)$, through a formula derived in elementary geometrical optics:[13]

$$S(r) = \frac{k(r) f(r) - r}{f(r)}, \tag{13}$$

where

$$k(r) = \int_{r_0}^{r} \left(\frac{\sqrt{f^2 + 1}}{f} - \frac{r f'}{f^2} \right) dr. \tag{14}$$

We may have to scale the shape if it is to represent the physical dimensions of the mirror.

5. VALIDATION OF THE METHOD: DEWARPING A PHOTOGRAPH OF A MODERN CONVEX MIRROR

Here we test the above methods by applying them to a photograph of a modern convex mirror of known shape. Figure 2 shows the front view of the ceiling-mounted convex mirror taken by a digital camera. We applied simple digital edge-detecting filters to the full image, then hand selected the resulting contours that correspond to straight lines in the source scene. While our method also permits us to enter discrete points known to be colinear in the scene, there was no need to search for such points in this image. Likewise, our method allows us to identify disjoint segments of a single partially occluded line but there were no examples of such occluded lines in this photograph.

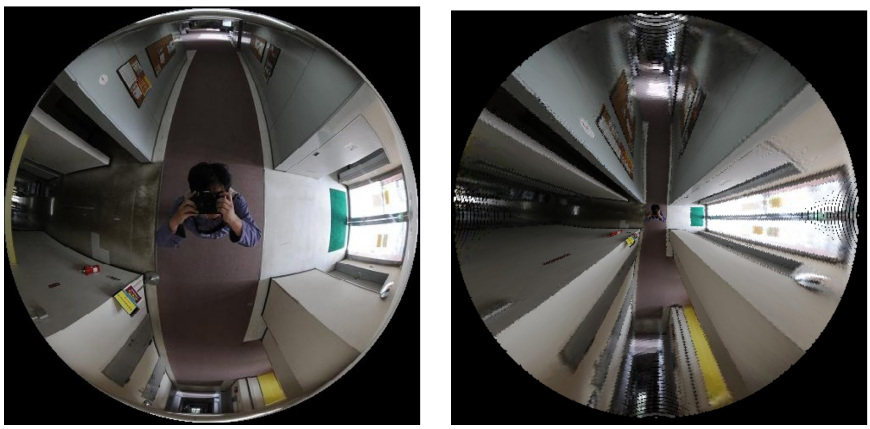

Figure 2. Left: An axial photograph of a modern ceiling mounted convex surveillance mirror in the hallway of an office walkway. Right: The image dewarped by our methods. Notice the straightness of the lines throughout the image.

Our basis set $f_n(r)$ consisted of polynomials up to 6th order and we estimated the dewarping function to be $f(r) = r + 0.997r^4 + 4.002r^6$. The image could be dewarped with a single overall function and did not require the interpolation methods described in Sect. 3. The estimated mirror shape, derived from $f(r)$ according to Eqs. 13 and 14, is very similar to the original physical shape, as shown in Fig. 3. In this estimation the peripheral area is not inferred because the method only covers the image data, which corresponds to a field of view in the scene of 180°.

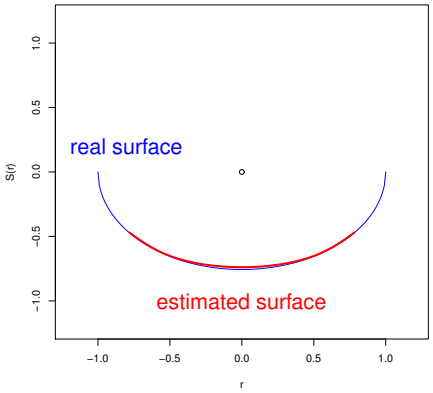

Figure 3. The surface of the real mirror measured in situ (blue), and estimated by our methods (red). (The estimated surface extends only to the section providing a 180° field of view in the scene.) There is excellent agreement between the estimated and actual surface.

6. APPLICATION TO ARTWORK

We applied our method to depictions of convex mirrors in important works of wester art: Johannes van Eyck's *Portrait of Giovanni (?) Arnolfini and his wife*, an important masterpiece from the early Renaissance, and Parmigianino's *Self portrait in a convex mirror*, an early work in the Mannerist tradition.

Johannes van Eyck, *Portrait of Giovanni (?) Arnolfini and his wife* (1434)

The centrally placed mirror in van Eyck's work is perhaps the most famous mirror of any type in western art. It symbolically represents the omniscient God overseeing the wedding, and reveals the room and windows, the back of Arnolfini and his wife as well as the two witnesses to the wedding, entering through the door.[14] We used the methods described in Sects. 2 and 3 with linear and trigonometric basis functions. We found that no single simple dewarping function gave superb results throughout the entire image. Accordingly, we split the into a central disk and an outer annular region, divided at $r = 0.84$, with the component interpolation function shown in Fig. 4, determined empirically. Our results are summarized here:

$$\begin{aligned} f_1(r) &= -0.907r + 0.421\sin(\pi r/2) \\ f_2(r) &= 1.000r + 0.0269\tan(\pi r/2) \\ g_i(r) &= \frac{N_i(r)}{N_1(r) + N_2(r)}, \quad i = 1, 2 \\ N_1 &\sim N(0,1), \quad N_2 \sim N(1, 0.06) \\ f(r) &= g_1(r)\frac{f_1(r)}{f_1(0.84)} + g_2(r)\frac{f_2(r)}{f_2(0.84)}. \end{aligned} \tag{15}$$

The function f_1 yields an acceptable dewarping for the center of the image, such as the figures, and f_2 yields an acceptable dewarping for the outer annulus, such as the window sash and bed. We connected the two functions

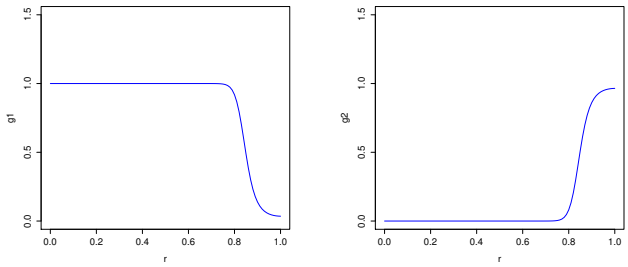

Figure 4. The weighted Gaussian components, $g_1(r)$ and $g_2(r)$, for interpolating the dewarping function throughout the full Arnolfini mirror image, for the empirically estimated transition point of $r = 0.84$.

at normalized distance $r = 0.84$, roughly between the outmost window sash and the middle part of the window. Figure 5 shows our results.

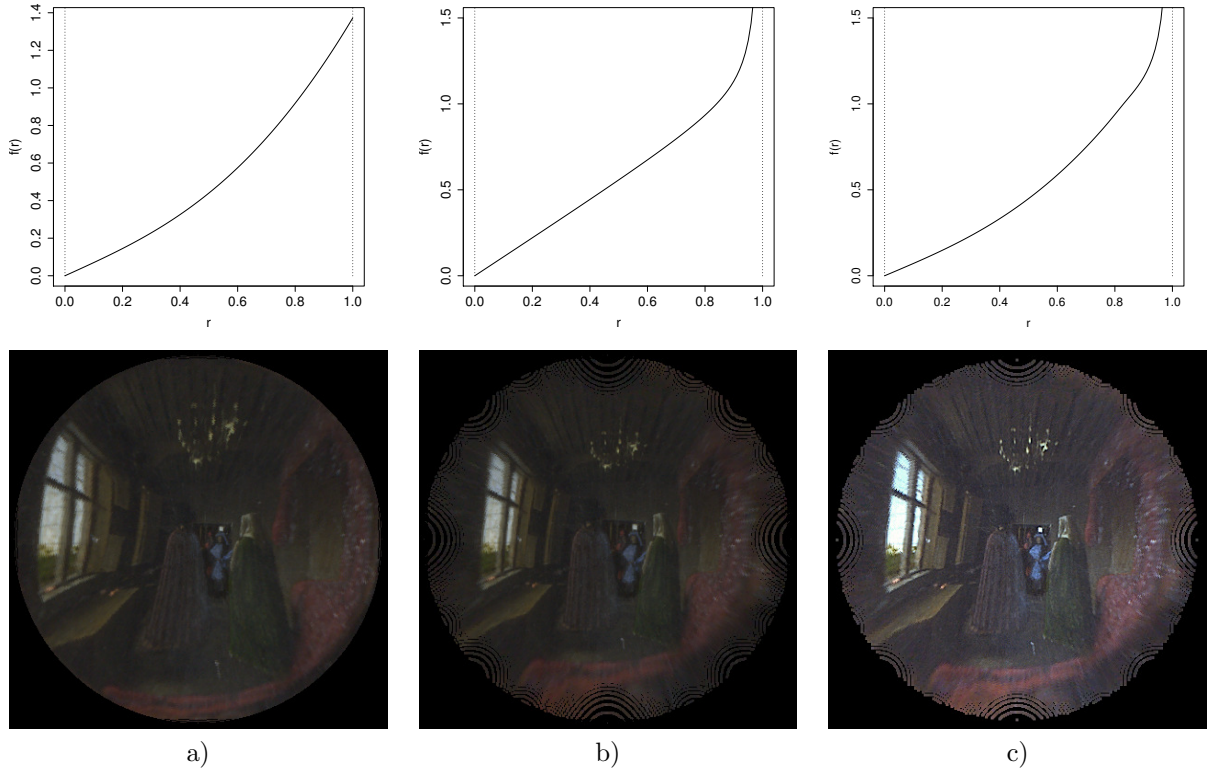

Figure 5. Dewarpings of the image in the mirror in Johannes van Eyck's *Portrait of Giovanni (?) Arnolfini and his wife* (1434), detail, 4.7 × 4.7 cm, using the values listed in Eq. 15. a) The dewarping function $f_1(r)$, plotted above, leads to excellent reconstruction in the center of the mirror, such as the doorway and figures, but leaves the periphery inadequately corrected, as can be seen in the window and bed. b) The dewarping function $f_2(r)$ rectifies the periphery well, but not the central disk. c) The full dewarping function, $f(r)$—a Gaussian weighting of $f_1(r)$ and $f_2(r)$—leads to excellent recovery of the shape of the full room.

We now turn to interpreting the dewarped *Arnolfini* image and the inferred mirror. Figure 6 shows a perspective analysis of the final dewarped image. Note that although our method straightens lines it does not impose other geometric coherence. Thus the geometric coherence in the dewarped image—definition of

Figure 6. A simple perspective analysis of the optimally dewarped full *Arnolfini* image shows excellent agreement of the vanishing point defined by the ceiling beams, and by the window and bench, though these two vanishing points are separated by a small but statistically significant non-zero distance. The geometric coherence and consistency here is superior to that in previous dewarping,[1] and this suggests that van Eyck depicted the image in his mirror more accurately than has been previously believed; it was just that his mirror deviated from an ideal sphere or paraboloid.

vanishing points, fidelity of objects of known shape, etc.—is a semi-independent test of the accuracy of the artist in reproducing what he saw in the mirror. (Note that such tests do not rely on an *assumption* that the artist strove for an accurate or "photographic" rendering, but rather *reveal* such accuracy.)

The high geometric coherence of the dewarped image sheds light on another problem in the interpretation of this painting. Paintings, especially from this period, are constructed objects, not mere "photographic" reproductions of the scenes before the artist.[14] Scholars have debated whether the Arnolfini tableau or is in part "fictive," a creation of van Eyck's imagination. While artists of that time were surely able to render a convincing fictive space (even if its perspective was inaccurate, as in the *Arnolfini portrait*), and could likely render such a fictive space as viewed from a new position and orientation (such as from the rear wall), it would have been an astounding visual and artistic accomplishment for van Eyck to have rendered a fictive room from a new position and as reflected in a convex mirror such that, when rectified, the geometry was as coherent and accurate as we find in Fig. 6. Of course details within the painting may differ from the tableau before him—such as the colors of the costumes, dressing of the bed, and so on. Nevertheless, we conclude that van Eyck worked from an actual room referent, and was not, generally speaking, depicting a fictive room of his imagination.

Figure 7 shows the estimated mirror surface and the best-fit paraboloid and the best-fit sphere. The focal length, in the paraxial-ray approximation, is half the radius of curvature, $f = R/2$, and remains close to that computed by previous methods.[3,4] Our new results show that the mirror shape deviated from a paraboloid, and so the smallest blur spot (the image of a point source) was even larger than found in earlier research. In short, if this mirror had been turned around and used as a projection mirror, then any resulting image would have been too blurry to use for tracing. (There are many other physical reasons such a mirror could not have been used as a projection mirror.[15]) These two new results confirm an indeed strengthen previous rebuttals to the claim by David Hockney and Charles Falco that "van Eyck placed a convex mirror at the center of this [Arnolfini] masterpiece, *the very mirror* which, turned around, he may well have used to construct the image"(emphasis added).[6] Our results also comport with, and indeed strengthen, the more general and broad scholarly rejection of the claim artists as early as 1430 traced optically projected images. [5, and references therein]

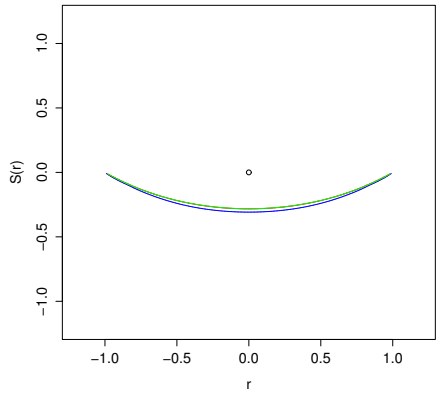

Figure 7. The surface of the mirror inferred from the *Arnolfini portrait* (blue) differs in slight, but apparent ways from the best-fit sphere (green). The curvature and thus focal length of the inferred mirror is similar to that in earlier research but the blur spot is larger. Thus, if this mirror were turned around and used as a projection mirror for the image in the painting including the chandelier, as has been proposed by others,[6] the image would have been too blurry to reveal such detail.

Parmigianino, *Self portrait in a convex mirror* (1523)

According to Vasari, Parmigianino produced this self portrait by working from a barber's convex mirror. The support is a section of a wooden sphere, which Stork and Furuichi showed using computer graphics reconstruction has a surface curvature consistent with that of a plausible convex mirror.[8] Such computer graphics methods provide greater flexibility than physical reconstructions of tableaus.[16]

Figure 8 shows the work and our dewarped image. The tableau has low-contrast, but clear lines corresponding to the line joining the rear wall and celing, the ceiling beams, window, and so forth. However, these lines are along the periphery of just one side of the work, far sparser than other images we have dewarped. Moreover, the location of the artist's eyes (including his presumably dominant right eye) is not in the center of the mirror, which would best justify our assumptions of radial warping, and this might introduce a slight inaccuracies.

Our dewarping function is described here:

$$\begin{aligned} f(r) &= g_1(r)f_1(r) + 3g_2(r)f_2(r) \\ f_1(r) &= 2.22x^8 + 0.637\sin(\pi r/2) \\ f_2(r) &= 0.504\sin(\pi r/2) + 0.133\tan(\pi r/2) \\ g_i &= \frac{N_i}{N_1 + N_2}, \quad i = 1, 2 \\ N_1 &\sim N(0, 0.88), \quad N_2 \sim N(1, 0.035). \end{aligned} \tag{16}$$

This new dewarped Parmigianino image bears some similarities to the image derived by Stork and Furuichi using computer graphics.[8] That previous work relied upon the construction of a three-dimensional computer graphics model and adjustment of spherical mirror. As such, that dewarping problem was somewhat underconstrained or formally ill posed, since many three-dimensional models could, in principle, be consistent with the final image. The dewarped fingers in the current method are somewhat long and ill-formed, likely because they lie far from the mirror's axis and the dewarping is most extreme. The relative size of the hand and head seems more commensurate with the close effective viewing position as well.

Figure 8. Left: Parmigianino, *Self portrait in a convex mirror*, oil on spherically domed wood panel, 24.4 cm diameter (Kunsthistorisches Museum, Vienna). Right: The dewarped image reveals straight lines, as guaranteed by the algorithm. The (central) face is not changed significantly.

7. CONCLUSIONS

We have demonstrated a non-iterative, principal-component-based method for computationally dewarping the images depicted in realist art. Our method affords greater flexibility and power than previous methods and can reveal the shape of the mirror itself, even if that shape differs from some ideal form such as a sphere or paraboloid. Our method dewarps the image in the *Arnolfini* mirror that is more spatially coherent than do previous approaches and yields an estimate of the mirror surface itself. The coherence of vanishing points provides a semi-independent measure of the accuracy of the van Eyck in rendering the virtual image before him. This coherence strongly supports the claim that van Eyck worked from an actual tableau as referent, not a fictive space. The inferred shape of the mirror does not differ significantly from that inferred by previous work, and thus their focal lengths are nearly the same as well. As such, our current work supports the conclusion of earlier research rejecting the claim of Hockney and Falco that the Arnolfini mirror could have been turned around and used as a projection mirror for the full image in the painting.

There remain limitations of our method. If there are no straight lines or colinear points in the scene, then our method our method would have to be modified to work with shapes of a known or assumed form. Our method works best if the view is along the axis of the mirror, but many mirrors are viewed from off the axis of symmetry. For instance, George W. Lambert's *The convex mirror* (c. 1916) in the National Gallery of Australia is a compelling and detailed rendition of an early 20th-century interior, with the artist's face at the periphery. Another general problem is a more principled method for choosing basis functions, spherical, parabolic, or other form—a topic of ongoing research.

Finally, we believe we have further demonstrated the value of rigorous, computer vision techniques for addressing problems in the history of art.[17,18]

Acknowledgments

We would like to thank Antonio Criminisi (Microsoft Research, Cambridge), Walter Liedtke (Metropolitan Museum of Art) and Robert Wald (Kunsthistorishes Museum) for helpful comments. The second author would like to thank the Getty Research Center for extended reader's privileges in its excellent library collection.

REFERENCES

1. A. Criminisi, M. Kemp, and S.-B. Kang, "Reflections of reality in Jan van Eyck and Robert Campin," *Historical methods* **3**(37), pp. 109–121, 2004.
2. D. S. Falk, D. R. Brill, and D. G. Stork, *Seeing the Light: Optics in nature, photography, color, vision and holography*, Wiley, New York, NY, 1986.
3. D. G. Stork, "Optics and realism in Renaissance art," *Scientific American* **291**(6), pp. 76–84, 2004.
4. D. G. Stork, "Optics and the old masters revisited," *Optics and Photonics News* **15**(3), pp. 30–37, 2004.
5. D. G. Stork, J. Collins, M. Duarte, Y. Furuichi, D. Kale, A. Kulkarni, M. D. Robinson, C. W. Tyler, S. Schechner, and N. Williams, "Did early Renaissance painters trace optically projected images? The conclusion of independent scientists, art historians and artists," in *Digital imaging for cultural heritage preservation*, F. Stanco, S. Battiato, and G. Gallo, eds., pp. 379–407, CRC Press, (Boca Raton, FL), 2011.
6. `www.webexhibits.org/hockneyoptics`.
7. S. Savarese, R. Spronk, D. G. Stork, and A. DelPozo, "Reflections on praxis and facture in a devotional portrait diptych: A computer analysis of the mirror in Hans Memling's *Virgin and Child and Maarten van Nieuwenhove*," in *Computer image analysis in the study of art*, D. G. Stork and J. Coddington, eds., **6810**, pp. 68100G–1–10, SPIE/IS&T, Bellingham, WA, 2008.
8. D. G. Stork and Y. Furuichi, "Reflections on Parmigianino's *Self portrait in a convex mirror*: A computer graphics reconstruction of the artist's studio," in *Computer image analysis in the study of art II*, D. G. Stork, J. Coddington, and A. Bentkowska-Kafel, eds., **7531**, pp. 75310J1–9, SPIE/IS&T, Bellingham, WA, 2010.
9. S. Savarese, M. Chen, and P. Perona, "Local shape from mirror reflections," *International Journal of Computer Vision* **64**(1), pp. 31–67, 2005.
10. H. Hino, Y. Usami, J. Fujiki, S. Akaho, and N. Murata, "Calibration of radially symmetric distortion fitting principal component," in *Proceedings of the 13th Conference on Computer Analysis of Images and Patterns*, X. Jiang and N. Petkov, eds., **LNCS 5702**, pp. 149–156, (Münster, Germany), 2009.
11. J. Fujiki, H. Hino, Y. Usami, S. Akaho, and N. Murata, "Self-calibration of radially symmetric distortion by model selection," in *International Conference on Pattern Recognition (ICPR)*, pp. 1812–1815, (Istambul, Turkey), 2010.
12. R. O. Duda, P. E. Hart, and D. G. Stork, *Pattern classification*, John Wiley and Sons, New York, NY, Second ed., 2001.
13. M. V. Klein, *Optics*, John Wiley and Sons, New York, NY, 1970.
14. C. Harbison, *Jan van Eyck: The play of realism*, Reaktion Books, New York, NY, 1997.
15. S. J. Schechner, "Between knowing and doing: Mirrors and their imperfections in the Renaissance," in *Early Science and Medicine: A Journal for the Study of Science, Technology and Medicine in the Pre-modern Period: Optics, instruments and painting 1420–1720: Reflections on the Hockney-Falco Thesis*, S. Dupré, ed., **X, no. 2**, pp. 137–162, Brill Academic Publishers, Leiden, The Netherlands, 2005.
16. S. Ferino-Pagden, "Parmigianinos Selbstportrait: Materie und Reflex," in *Parmigianino und der europäische Manierismus*, S. Ferino-Pagden and L. F. Schianchi, eds., pp. 43–55, Ginko Press, (Vienna, Austria), 2003.
17. D. G. Stork and J. Coddington, eds., *Computer image analysis in the study of art*, vol. 6810, SPIE/IS&T, Bellingham, WA, 2008.
18. D. G. Stork, J. Coddington, and A. Bentkowska-Kafel, eds., *Computer vision and image analysis in the study of art*, vol. 7531, SPIE/IS&T, Bellingham, WA, 2010.